Effect of Local Thermal Nonequilibrium on the Stability of Natural Convection in an Oldroyd-B Fluid Saturated Vertical Porous Layer

B. M. Shankar[1]
Department of Mathematics,
PES University,
Bangalore 560 085, India
e-mail: bmshankar@pes.edu

I. S. Shivakumara
Department of Mathematics,
Bangalore University,
Bangalore 560 056, India

The effect of local thermal nonequilibrium (LTNE) on the stability of natural convection in a vertical porous slab saturated by an Oldroyd-B fluid is investigated. The vertical walls of the slab are impermeable and maintained at constant but different temperatures. A two-field model that represents the fluid and solid phase temperature fields separately is used for heat transport equation. The resulting stability eigenvalue problem is solved numerically using Chebyshev collocation method as the energy stability analysis becomes ineffective in deciding the stability of the system. Despite the basic state remains the same for Newtonian and viscoelastic fluids, it is observed that the base flow is unstable for viscoelastic fluids and this result is qualitatively different from Newtonian fluids. The results for Maxwell fluid are delineated as a particular case from the present study. It is found that the viscoelasticity has both stabilizing and destabilizing influence on the flow. Increase in the value of interphase heat transfer coefficient H_1, strain retardation parameter Λ_2 and diffusivity ratio α portray stabilizing influence on the system while increasing stress relaxation parameter Λ_1 and porosity-modified conductivity ratio γ exhibit an opposite trend. [DOI: 10.1115/1.4035199]

Keywords: stability, vertical porous layer, heat transfer, Chebyshev collocation method, eigenvalue problem

1 Introduction

The interaction of destabilizing buoyancy forces and stabilizing viscous forces on the stability of fluid flows in porous media has been the subject of intensive research interest as many geophysical and technological phenomena are maintained by these forces. In his classical paper, Gill [1] investigated analytically the stability properties of natural convection in a vertical layer with reference to Darcy's flow of a Newtonian fluid for which one boundary is uniformly cold and the other is uniformly hot. Subsequently, Rees [2] considered the same problem as Gill but included the Prandtl–Darcy term (a time derivative of the velocity) in the momentum equation, while Lewis et al. [3] quantified Gill's results by determining how quickly the disturbances decay. Straughan [4] and Qin and Kaloni [5] used energy methods to give sufficient conditions for the stability of convection in a vertical porous slab. Barletta and Alves [6] extended the analysis developed by Gill [1] to the case of a power-law fluid and observed that the instability does not occur for such a non-Newtonian fluid. All these investigators considered the local thermal equilibrium (LTE) model where a single temperature equation is used to describe the heat transport processes.

As highlighted by several authors (Vafai and Sozen [7], Minkowycz et al. [8], Duval et al. [9], Rees and Pop [10], and Rees [11]), the condition of LTE requires numerous constraints and this assumption is no longer valid when the particles or pores are not small enough, when the thermal properties differ widely, or when the convective transport is important. This suggests the inevitability of LTNE effects in the study of thermal convection in porous media. The LTNE model encompasses a two-field model for heat transport equation each representing the fluid and solid phases separately. Studies carried out on forced and free convection in fluid saturated porous media using LTNE model are amply documented in the book by Nield and Bejan [12]. Thermal instability in porous media using a LTNE model attracted the attention of researchers in the recent past (Banu and Rees [13], Malashetty et al. [14], Shivakumara et al. [15], Straughan [16], Celli et al. [17], Barletta and Rees [18], and Barletta et al. [19]).

However, studies on the stability of thermal convection in a vertical porous layer with LTNE model are very scanty. Rees [20] and Scott and Straughan [21] presented a new perspective on Gill's problem by taking into account of the LTNE effect. These authors confirmed the conclusion that the basic flow is stable with either linear (Rees [20]) or nonlinear (Scott and Straughan [21]) stability analyses. Other important works on this topic have been well documented in the book by Straughan [22]. Majority of the investigations are based on Newtonian fluids, but many fluids display non-Newtonian characteristics and this has prompted researchers to consider non-Newtonian effects depending on the situations. For example, a polymer melt shows time-independent (shear-thinning) and viscoelastic behaviors simultaneously and a china clay suspension may exhibit a combination of time-independent (shear-thinning or shear-thickening) and time-dependent (thixotropic) features at certain concentrations and/or at appropriate shear rates. Thus, there exist different kinds of non-Newtonian fluids and their behavior is different from one another. In other words, non-Newtonian fluids do not lend themselves to a

[1]Corresponding author.

Contributed by the Heat Transfer Division of ASME for publication in the Journal of Heat Transfer. Manuscript received June 1, 2016; final manuscript received November 4, 2016; published online January 18, 2017. Assoc. Editor: Dr. Antonio Barletta.

unified treatment like Newtonian fluids. In particular, the flow of viscoelastic fluids has received considerable attention of researchers because of their importance in plethora of engineering applications [23].

Thermal convective instability in a horizontal viscoelastic fluid layer heated from below and also its counterpart in a layer of porous medium has been extensively investigated (Li and Khayat [24], Sheu et al. [25], and Malashetty and Kulkarni [26]). The stability of natural convection in a vertical layer of viscoelastic liquid was considered by Gozum and Arpaci [27], who treated the case of a Maxwell liquid while Takashima [28] investigated the problem for Oldroyd-B liquid, but the stability of the flow of such liquids saturating porous media has not been investigated and reported in the open literature. The purpose of the present investigation is to consider the effects of LTNE and viscoelasticity on the stability of natural convection in a vertical layer of Darcy porous medium. The flow system considered and the mathematical model adopted are exactly the same as those assumed by Rees [20], but the difference is that the fluid is a polymeric solution obeying the Oldroyd-B equation. The eigenvalue problem is solved numerically using Chebyshev collocation method. The results for the Maxwell fluid are also obtained as a particular case from the present study. Our numerical study suggests that the linearly stable behavior found by Rees [20] for Newtonian fluids does not apply for viscoelastic fluids despite the basic state remains the same for these two types of fluids.

This paper is organized as follows. The formulation of the problem including the governing equations and the nondimensionalization is outlined in Sec. 2. Linear stability analysis is given in Sec. 3, the numerical method employed to solve the stability equations is described in Sec. 4. Results as well as discussion of the numerical solutions are given in Sec. 5. The main conclusions from this study are summarized in Sec. 6.

2 Mathematical Formulation

The physical configuration of the problem is illustrated schematically in Fig. 1. We consider an Oldroyd-B fluid-saturated vertical layer of Darcy porous medium of width, $2d$. A Cartesian coordinate system (x, y, z) is chosen with the origin in the middle of the vertical porous layer, where the x-axis is taken perpendicular to the plates and the z-axis is vertically upwards, opposite to the direction of gravity. The plate at $x = -d$ is kept at a uniform temperature T_1, while the plate at $x = d$ is maintained at uniform temperature $T_2\,(> T_1)$. The LTNE model is invoked which is based on the definition of two different local temperatures, one for the solid phase and one for the fluid phase. The interphase heat transfer rate is modeled through a constant coefficient h multiplying the local temperature difference between the phases. Thus, separate energy balance equations for each phase have been considered.

The governing equations under the Oberbeck–Boussinesq approximation are [20,29,30]

$$\nabla \cdot \mathbf{q} = 0 \tag{1}$$

$$\left(1 + \lambda_1 \frac{\partial}{\partial t}\right)(\nabla p - \rho_f \mathbf{g}) = -\frac{\mu}{K}\left(1 + \lambda_2 \frac{\partial}{\partial t}\right)\mathbf{q} \tag{2}$$

$$\varepsilon(\rho c)_f \frac{\partial T_f}{\partial t} + (\rho c)_f (\mathbf{q} \cdot \nabla) T_f = \varepsilon \kappa_f \nabla^2 T_f + h(T_s - T_f) \tag{3}$$

$$(1 - \varepsilon)(\rho c)_s \frac{\partial T_s}{\partial t} = (1 - \varepsilon)\kappa_s \nabla^2 T_s - h(T_s - T_f) \tag{4}$$

$$\rho_f = \rho_0\{1 - \beta(T_f - T_0)\} \tag{5}$$

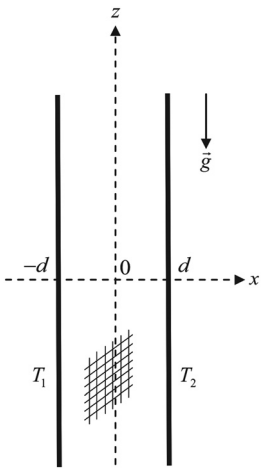

Fig. 1 Physical configuration

where $\mathbf{q} = (u, v, w)$ is the velocity vector, p is the pressure, λ_1 and λ_2 are stress relaxation and strain retardation time constants, respectively, ρ_f is the fluid density, ε is the porosity of the medium, $\mathbf{g}$ is the acceleration due to gravity, μ is the viscosity of the fluid, K is the permeability, T_f is the temperature of the fluid, T_s is the temperature of the solid, h is the interphase heat transfer coefficient, β is the thermal expansion coefficient, and ρ_0 is the density at reference temperature $T = T_0$ (at the middle of the channel). The Oldroyd-B constitutive relation is satisfied for fluids composed of a Newtonian solvent and a polymeric solute with viscosities μ_s and μ_p, respectively. The viscosity of the solution is given by $\mu = \mu_s + \mu_p$ and hence the ratio $\lambda_2/\lambda_1 = \mu_s/(\mu_s + \mu_p)$ is always less than or equal to unity (Akhatov and Chembarisova [31], Bird et al. [32], and Hirata et al. [33]). It is seen that Eq. (2) is simplified to Darcy's law for the flow of viscous Newtonian fluid through a porous medium when λ_1 and λ_2 assume the same value. The quantities are made dimensionless by scaling velocity by $\varepsilon\kappa_f/d$, length by d, pressure by $\varepsilon\mu\kappa_f/K$, time by d^2/κ_f, and temperature of the fluid and solid by $\Delta T\,(\Delta T = T_2 - T_1)$ to get

$$\left(1 + \Lambda_1 \frac{\partial}{\partial t}\right)\left(\nabla P - R_D T_f \hat{k}\right) = \left(1 + \Lambda_2 \frac{\partial}{\partial t}\right)\mathbf{q} \tag{6}$$

$$\frac{\partial T_f}{\partial t} + (\mathbf{q} \cdot \nabla) T_f = \nabla^2 T_f + H_t(T_s - T_f) \tag{7}$$

$$\alpha \frac{\partial T_s}{\partial t} = \nabla^2 T_s + H_t \gamma (T_f - T_s) \tag{8}$$

where P is the modified pressure, $R_D = \rho_0 g \beta \Delta T K d/\varepsilon\mu\kappa_f$ is the Darcy–Rayleigh number, $H_t = hd^2/\varepsilon\kappa_f$ is the scaled interphase heat transfer coefficient, $\Lambda_1 = \lambda_1\kappa_f/d^2$ is the relaxation parameter, $\Lambda_2 = \lambda_2\kappa_f/d^2$ is the retardation parameter, $\gamma = \varepsilon\kappa_f/(1 - \varepsilon)\kappa_s$ is the porosity-modified conductivity ratio, and $\alpha = (\rho c)_s\kappa_f/(\rho c)_f\kappa_s$ is the diffusivity ratio.

Taking curl on both sides of Eq. (6) to eliminate the pressure term and introducing the stream function $\psi(x, z, t)$ through

$$(u, 0, w) = \left(-\frac{\partial \psi}{\partial z}, 0, \frac{\partial \psi}{\partial x}\right) \tag{9}$$

the governing Eqs. (6)–(8) become

$$R_D\left(1+\Lambda_1\frac{\partial}{\partial t}\right)\frac{\partial T_f}{\partial x}=\left(1+\Lambda_2\frac{\partial}{\partial t}\right)\left(\frac{\partial^2\psi}{\partial x^2}+\frac{\partial^2\psi}{\partial z^2}\right) \tag{10}$$

$$\frac{\partial T_f}{\partial t}+\frac{\partial\psi}{\partial x}\frac{\partial T_f}{\partial z}-\frac{\partial\psi}{\partial z}\frac{\partial T_f}{\partial x}=\frac{\partial^2 T_f}{\partial x^2}+\frac{\partial^2 T_f}{\partial z^2}+H_t(T_s-T_f) \tag{11}$$

$$\alpha\frac{\partial T_s}{\partial t}=\frac{\partial^2 T_s}{\partial x^2}+\frac{\partial^2 T_s}{\partial z^2}+H_t\gamma(T_f-T_s) \tag{12}$$

The boundaries are impermeable and the appropriate boundary conditions are

$$\begin{aligned}&\psi=0,\ T_f=T_s=-1\ \text{ at }\ x=-1\\&\psi=0,\ T_f=T_s=1\ \text{ at }\ x=1\end{aligned} \tag{13}$$

3 Linear Stability Analysis

The basic state is a fully developed, unidirectional, steady, and laminar flow. Thus

$$\psi=\psi_b(x),\ T_f=T_{fb}(x),\ T_s=T_{sb}(x) \tag{14}$$

where the subscript b denotes the basic state. The basic state solution is found to be

$$\psi_b(x)=\frac{R_D}{2}(x^2-1),\ T_{fb}=x=T_{sb} \tag{15}$$

and it is same as that for an ordinary Newtonian fluid. To study the linear stability of fluid flow, we superimpose an infinitesimal disturbance on the base flow in the form

$$\psi=\psi_b(x)+\psi',\quad T_f=T_{fb}+T_f',\quad T_s=T_{sb}+T_s' \tag{16}$$

Substituting Eq. (16) into Eqs. (10)–(12) and using Eq. (15), we get

$$R_D\left(1+\Lambda_1\frac{\partial}{\partial t}\right)\frac{\partial T_f'}{\partial x}=\left(1+\Lambda_2\frac{\partial}{\partial t}\right)\left(\frac{\partial^2\psi'}{\partial x^2}+\frac{\partial^2\psi'}{\partial z^2}\right) \tag{17}$$

$$\frac{\partial T_f'}{\partial t}+R_D x\frac{\partial T_f'}{\partial z}-\frac{\partial\psi'}{\partial z}=\frac{\partial^2 T_f'}{\partial x^2}+\frac{\partial^2 T_f'}{\partial z^2}+H_t\left(T_s'-T_f'\right) \tag{18}$$

$$\alpha\frac{\partial T_s'}{\partial t}=\frac{\partial^2 T_s'}{\partial x^2}+\frac{\partial^2 T_s'}{\partial z^2}+H_t\gamma\left(T_f'-T_s'\right) \tag{19}$$

Employing the normal mode analysis procedure in which we look for the solution of the form

$$(\psi',T_f',T_s')=[\Psi(x),\Theta(x),\Phi(x)]e^{ia\,(z-ct)} \tag{20}$$

where c is the wave speed which is real and positive and a is the vertical wave number, we then obtain

$$(1-ia\Lambda_2 c)(D^2-a^2)\Psi=(1-ia\Lambda_1 c)R_D D\Theta \tag{21}$$

$$(D^2-a^2)\Theta+H_t(\Phi-\Theta)+ia\,\Psi-ia\,\Theta R_D x=-ia\,c\,\Theta \tag{22}$$

$$(D^2-a^2)\Phi+H_t\gamma(\Theta-\Phi)=-ia\,c\alpha\,\Phi \tag{23}$$

where $D=\partial/\partial x$.

The associated boundary conditions are

$$\Psi=\Theta=\Phi=0\quad\text{at}\quad x=\pm1 \tag{24}$$

4 Numerical Solution

Equations (21)–(23) together with the boundary conditions (24) constitute an eigenvalue problem. This resulting eigenvalue problem is solved numerically using the Chebyshev collocation method. The kth order Chebyshev polynomial is given by

$$\xi_k(x)=\cos k\tau,\quad \tau=\cos^{-1}x \tag{25}$$

The Chebyshev collocation points are given by

$$x_j=\cos\left(\frac{\pi j}{N}\right),\quad j=0(1)N \tag{26}$$

Here, the right and left wall boundaries correspond to $j=0$ and N, respectively. The field variables Ψ,Θ, and Φ can be approximated in terms of Chebyshev polynomials as follows:

$$\Psi(x)=\sum_{j=0}^{N}\xi_j(x)\Psi_j,\quad \Theta(x)=\sum_{j=0}^{N}\xi_j(x)\Theta_j,\quad \Phi(x)=\sum_{j=0}^{N}\xi_j(x)\Phi_j \tag{27}$$

The governing Eqs. (21)–(24) are discretized in terms of Chebyshev polynomials to get

$$\begin{aligned}&(1-iac\Lambda_2)\left(\sum_{k=0}^{N}B_{jk}\Psi_k-a^2\Psi_j\right)\\&\quad=(1-iac\Lambda_1)R_D\sum_{k=0}^{N}A_{jk}\Theta_k,\ j=1(1)N-1\end{aligned} \tag{28}$$

$$\begin{aligned}&ia\Psi_j+\left(\sum_{k=0}^{N}B_{jk}\Theta_k-a^2\Theta_j\right)+H_t(\Phi_j-\Theta_j)-iaxR_D\Theta_j\\&\quad=-iac\Theta_j,\ j=1(1)N-1\end{aligned} \tag{29}$$

$$\left(\sum_{k=0}^{N}B_{jk}\Phi_k-a^2\Phi_j\right)+H_t\gamma(\Theta_j-\Phi_j)=-iac\alpha\Phi_j,\quad j=1(1)N-1 \tag{30}$$

$$\Psi_0=\Psi_N=0 \tag{31}$$

$$\Theta_0=\Theta_N=0 \tag{32}$$

$$\Phi_0=\Phi_N=0 \tag{33}$$

where

$$A_{jk}=\begin{cases}\dfrac{c_j(-1)^{k+j}}{c_k(x_j-x_k)} & j\neq k\\[2ex] \dfrac{x_j}{2\left(1-x_j^2\right)} & 1\le j=k\le N-1\\[2ex] \dfrac{2N^2+1}{6} & j=k=0\\[2ex] -\dfrac{2N^2+1}{6} & j=k=N\end{cases} \tag{34}$$

Table 1 Comparison of Chebyshev collocation and Galerkin method for different values of Λ_1, Λ_2, and H_t when $\gamma = 0.5$ and $\alpha = 1$

			Chebyshev collocation method			Galerkin method		
Λ_1	Λ_2	H_t	R_{Dc}	a_c	c_c	R_{Dc}	a_c	c_c
0.5	0.1	10^{-5}	10.75850380	1.830	−11.46302302	10.75794663	1.830	−11.46281452
		10^{1}	15.81398289	2.172	−16.43627460	15.81271751	2.171	−16.43459972
		10^{2}	37.34996584	1.368	−19.44964635	37.35167643	1.368	−19.45115243
		10^{5}	32.28133166	1.830	−11.46980054	32.28491609	1.830	−11.46713105
0.3	0.1	10^{-5}	18.30266059	2.057	−18.35841787	18.30853947	2.057	−18.35339568
		10^{1}	26.91405207	2.392	−26.91462733	26.97341092	2.393	−26.91421528
		10^{2}	92.60956965	3.178	−87.95040743	92.59990138	3.176	−87.94876803
		10^{5}	54.95383282	2.056	−18.38073693	54.95728568	2.057	−18.37822848
0.5	0.2	10^{-5}	21.77219873	2.080	−21.08078599	21.77037544	2.080	−21.08513865
		10^{1}	32.27491763	2.422	−31.63818826	32.28549369	2.422	−31.64789253
		10^{2}	112.35995490	3.274	−108.23361316	112.32249317	3.272	−108.24967291
		10^{5}	65.39532279	2.079	−21.11554891	65.38605802	2.080	−21.11397806

and

$$B_{jk} = A_{jm} \cdot A_{mk} \tag{35}$$

with

$$c_j = \begin{cases} 2 & j = 0, N \\ 1 & 1 \le j \le N-1 \end{cases}$$

Equations (28)–(33) form the following system of linear algebraic equations:

$$AX = cBX \tag{36}$$

where c is the eigenvalue and X is the discrete representation of the eigenfunction; A and B are square (complex) matrices of order $3(N+1)$. The time representation in ψ, T_f, and T_s is employed in the form e^{-iact} with $c = c_r + ic_i$ which results in ψ, T_f, and T_s having terms of form $e^{-iac_r t} \cdot e^{ac_i t}$. The eigenvalues are found such that the largest value of c_i is zero and then the result is minimized over the wave number a. The resulting R_D value is then the critical Darcy–Rayleigh number with corresponding wave number. The value $c_i = 0$ is chosen because this is the threshold at which the solution becomes unstable according to linear theory. For example, if $c_i > 0$ then ψ, T_f, and T_s grow rapidly like $e^{ac_i t}$ and the solution is unstable.

5 Results and Discussion

The resulting generalized stability eigenvalue problem is solved numerically using Chebyshev collocation method. It is found that accurate solutions up to the sixth digit could be reached by taking ten terms in the Chebyshev collocation method and hence the results are obtained by taking $N = 10$. To confirm the results so obtained, the numerical computations are also carried out using the Galerkin method with Legendre polynomials as trial functions (Appendix A) for representative sets of parametric values. The results so obtained by taking ten terms in the Galerkin expansion are shown in Table 1 along with those obtained from the Chebyshev collocation method. From this table, it is seen that the results obtained from both the methods complement with each other. The numerical computations carried out reveal that the stability can be

Table 2 Variation of R_{Dc} and a_c as a function of Λ_1 and H_t when $\Lambda_2 = 0, \gamma = 0.5$, and α=1.

	$H_t = 10^{-5}$		$H_t = 1$	
Λ_1	R_{Dc}	a_c	R_{Dc}	a_c
10^{-2}	54.66697583	1.918	57.58228036	1.954
10^{-3}	55.14625932	2.159	57.94391180	2.202
10^{-4}	55.46833793	2.178	58.26674218	2.222
10^{-5}	55.50525578	2.180	58.30427522	2.224
10^{-6}	55.50899381	2.180	58.30807986	2.224

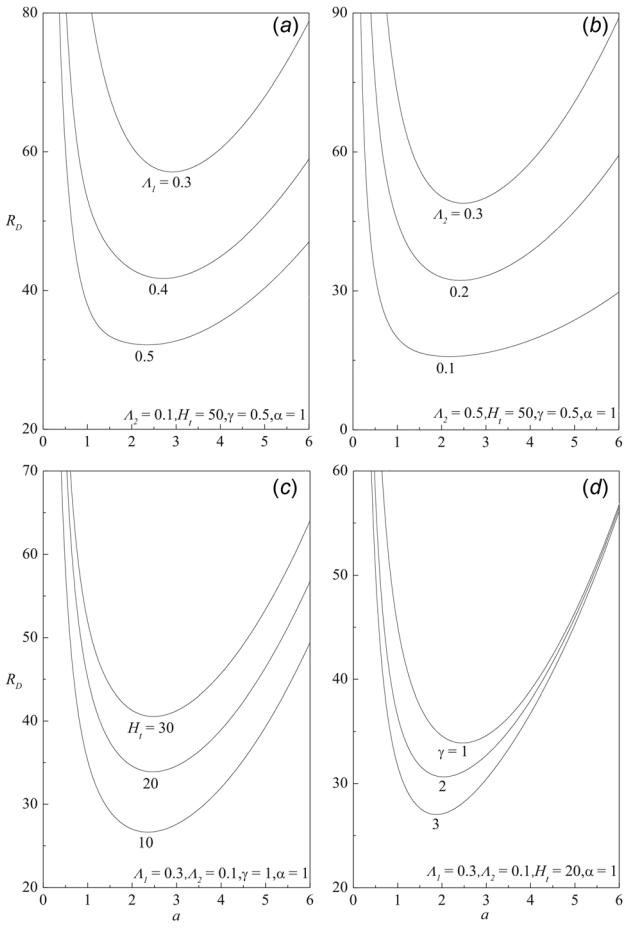

Fig. 2 Neutral stability curves

achieved only when $\Lambda_1 = \Lambda_2$ (Newtonian fluid) but not when Λ_1 is small enough (with $\Lambda_2 = 0$). The values of R_{Dc} tabulated in Table 2 for different Λ_1 and H_t when $\Lambda_2 = 0$, $\gamma = 0.5$ and $\alpha = 1$ justify this fact. To corroborate our numerically observed instability of the system in the presence of viscoelastic effects, the energy stability analysis of Rees [20] was followed and the details are given in Appendix B. From Eq. (B4), we retrieve the result obtained by Rees [20] when $\Lambda_1 = \Lambda_2$ which indicates that the basic flow is always stable in the case of Newtonian fluids as the growth rate of normal modes is always negative. The presence of viscoelastic effects, however, does not allow us to draw any such general conclusion on the stability of the system due to the presence of indecisive first term on the left-hand side of Eq. (B4).

The numerical computations reveal that the instability sets in always via oscillatory mode ($c_c \neq 0$) and the related oscillatory neutral stability curves on the (R_D, a) -plane for various values of Λ_1, Λ_2, H_t, and γ for a fixed value of $\alpha = 1$ are demonstrated in Fig. 2. The oscillatory neutral stability curves exhibit single but different minimum with respect to the wave number for various values of these physical parameters. The region below each neutral curve corresponds to the stable state of the system. Thus, we note that increasing Λ_1 (Fig. 2(*a*)) and γ (Fig. 2(*d*)) is to decrease the region of stability, while opposite is the trend with increasing Λ_2 (Fig. 2(*b*)) and H_t (Fig. 2(*c*)).

The critical Darcy–Rayleigh number R_{Dc}, the critical wave speed c_c, and the corresponding critical wave number a_c are computed for different values of physical parameters to know their impact on the stability characteristics of the system. Figure 3(*a*) shows the variation of R_{Dc} as a function of H_t for different values of stress relaxation parameter Λ_1 when $\Lambda_2 = 0.1$, $\gamma = 0.5$, and $\alpha = 1$. For $\Lambda_1 = 0.3$, the curve emanates from $R_{Dc} = 18.3$ and progresses constantly till $H_t = 0$. Subsequently, it faces a sharp

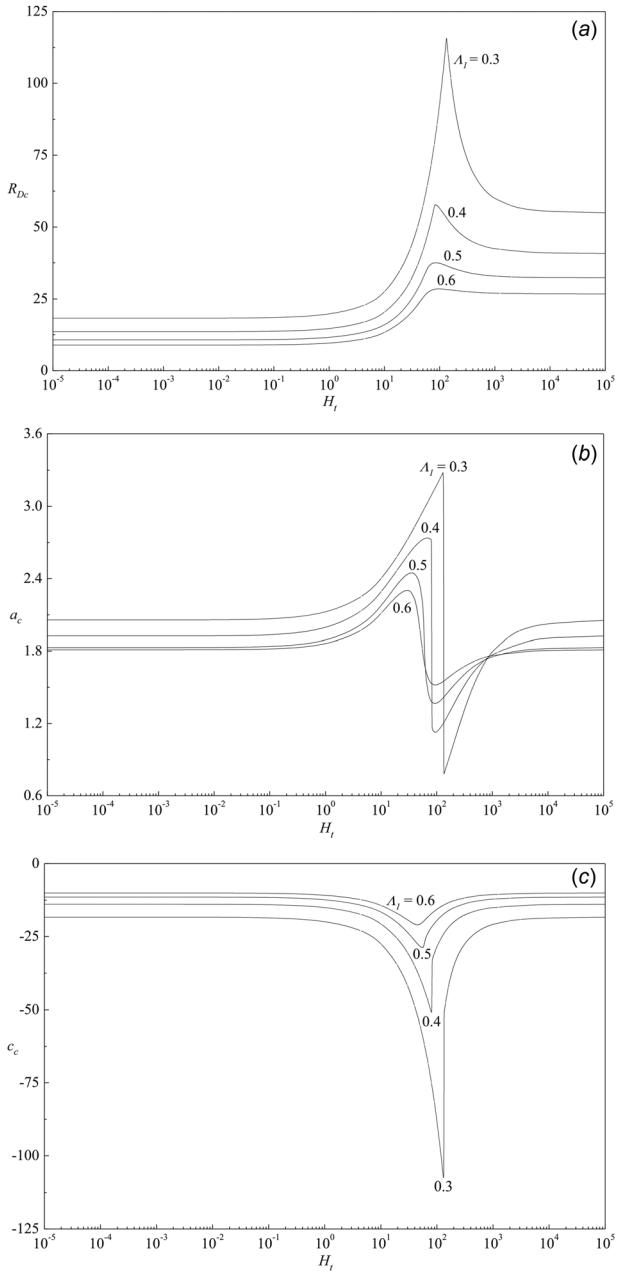

Fig. 3 Variation of (*a*) R_{Dc}, (*b*) a_c, and (*c*) c_c with H_t for various values of Λ_1 when $\Lambda_2 = 0.1, \gamma = 0.5$, and $\alpha = 1$

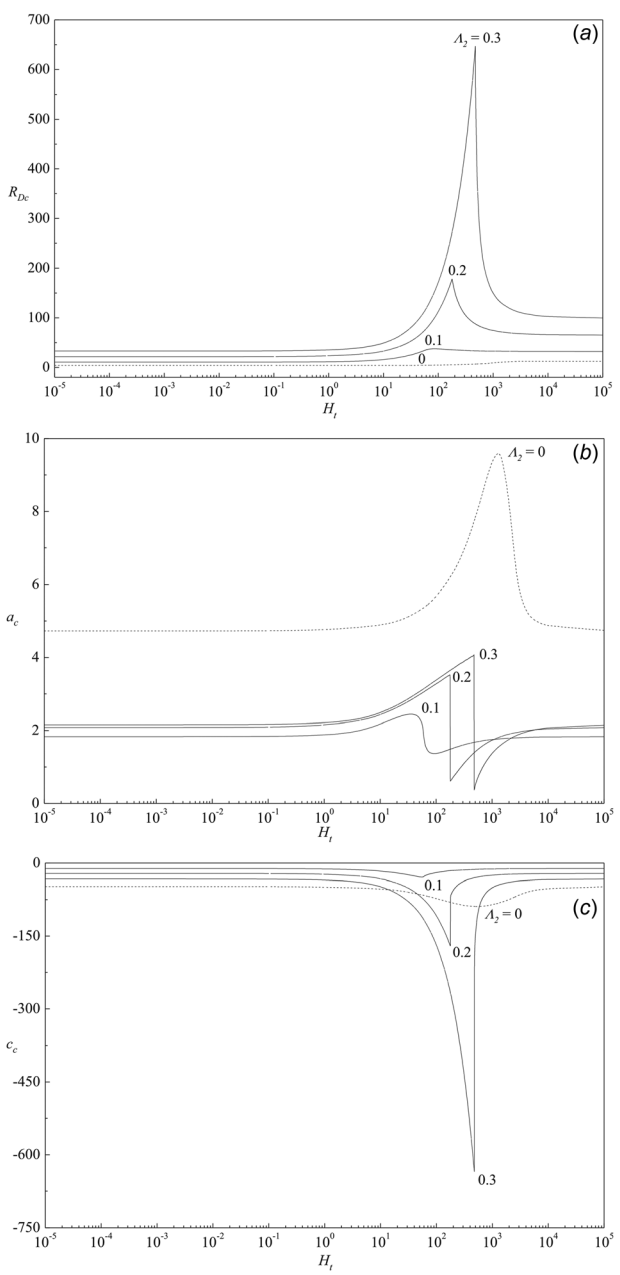

Fig. 4 Variation of (*a*) R_{Dc}, (*b*) a_c, and (*c*) c_c with H_t for various values of Λ_2 when $\Lambda_1 = 0.5, \gamma = 0.5$, and $\alpha = 1$

increase in its behavior, followed by a steep decline in the value of R_{Dc} with the increase in H_t. The curves for $\Lambda_1 = 0.4$, 0.5, and 0.6 initially progress constantly till $H_t = 1$ and further experience a gradual rise followed by a steady fall. All the curves reach their asymptotic state for values of $H_t \geq 1000$. It is noted that the effect of increase in the stress relaxation parameter Λ_1 is to decrease R_{Dc}, and thus, it has a destabilizing effect on the flow. This may be due to the fact that increase in Λ_1 amounts to allowing the applied stress to act for a longer time on the fluid element which results in lesser elastic memory of the fluid. In fact, the increase of relaxation ceases the stickiness of the fluid and hence the effect of friction will be lesser so that the convection sets in at lower values of R_{Dc}. Figure 3(*b*) is a plot of a_c versus H_t for different values of Λ_1 and it is seen that a_c moves toward a common limit as $H_t \to 0$ and $H_t \to \infty$ irrespective of the value of Λ_1. This is due to the fact that, for very small H_t, the solid phase ceases to affect the thermal field of the fluid. On the other hand, as $H_t \to \infty$, the solid and fluid phases have almost equal temperatures. For the intermediate values of H_t, a_c attains both maximum and minimum values. Besides, increase in Λ_1 is to increase the size of convection cells because its effect is to reduce the friction and to ease the fluid motion. Corresponding curves of c_c displayed in Fig. 3(*c*) show that the instability sets in only via oscillatory mode and also c_c approaches common limit as $H_t \to 0$ and $H_t \to \infty$ for all values of Λ_1 considered. It is observed that there is no variation in the value of c_c till $H_t = 1$ and then plummets as H_t increases to 100 but forthwith rise sharply and saturates as $H_t \to \infty$. The curve of $\Lambda_1 = 0.3$ experiences the maximum decline and attains a negative peak value of -109.2, whereas the curve of $\Lambda_1 = 0.6$ faces the minimum fall.

Figures 4(*a*) and 4(*b*) illustrate the variation of R_{Dc} and a_c as a function of H_t for different values of strain retardation parameter Λ_2 for $\Lambda_1 = 0.5$, $\gamma = 0.5$ and $\alpha = 1$. Figure 4(*a*) reveals that the origin of the plots increases on the R_{Dc} axis as the value of Λ_2 increases. The general pattern followed by all the plots is increasing peak as Λ_2 increases at the intermediate values of H_t, while

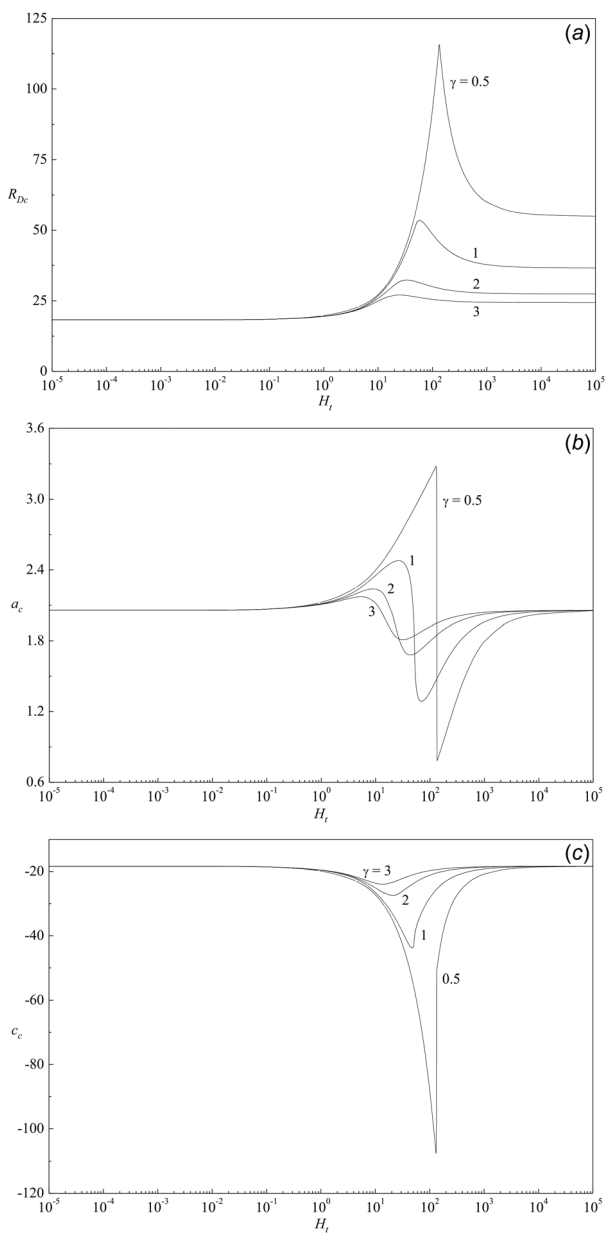

Fig. 5 Variation of (*a*) R_{Dc}, (*b*) a_c, and (*c*) c_c with H_t for various values of γ when $\Lambda_1 = 0.3, \Lambda_2 = 0.1$, and $\alpha = 1$

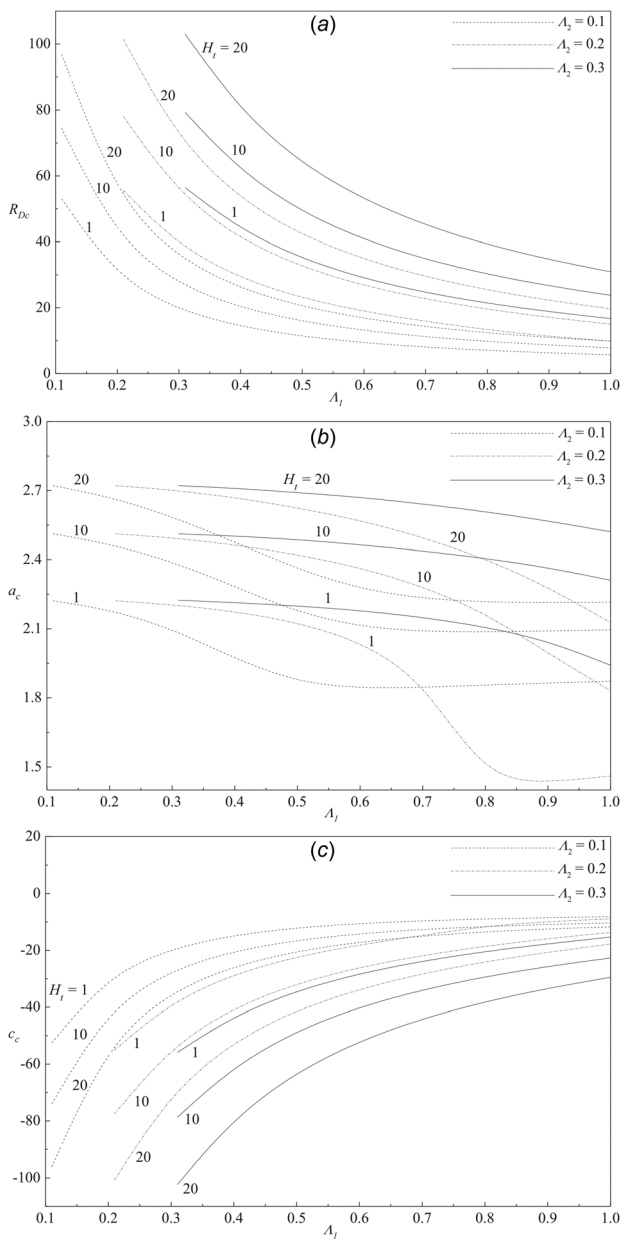

Fig. 6 Variation of (*a*) R_{Dc}, (*b*) a_c, and (*c*) c_c with Λ_1 for various values of H_t and Λ_2 when $\gamma = 0.5$, $\alpha = 1$

the effect of Λ_2 is of no consequence at lower and higher values of H_t. From Fig. 4(*a*), it is also obvious that an increase in the value of strain retardation parameter Λ_2 is to increase the value of R_{Dc} and shows a stabilizing effect on the system because increase in Λ_2 amounts to increase in the time taken by the fluid element to respond to the applied stress. That is, during the growth of retardation parameter, the effect of friction will be higher and as a result higher values of R_{Dc} are needed to instill instability on the system. Also, the curve of $\Lambda_2 = 0$ lies well below the curves of $\Lambda_2 \neq 0$ indicating that the elasticity of a Maxwellian fluid has a more destabilizing influence on the system as expected. Figure 4(*b*) demonstrates the variation in a_c with H_t for different values of Λ_2. It is seen that the critical wave numbers for $\Lambda_2 = 0$ (Maxwell fluid) are higher than those of $\Lambda_2 \neq 0$ (Oldroyd-B fluid) as there will be no friction on the fluid motion. For nonzero values of Λ_2, the critical wave number assumes both maximum and minimum values at intermediate values of H_t. Figure 4(*c*) illustrates the behavior of c_c as a function of H_t for different values of Λ_2.

The effect of different values of γ on R_{Dc}, a_c, and c_c is exhibited in Figs. 5(*a*)–5(c), respectively, as a function of H_t for $\Lambda_1 = 0.3$, $\Lambda_2 = 0.1$, and $\alpha = 1$. At lower values of H_t, it is observed that the values of R_{Dc} are closer to those of the LTE case, which are independent of γ. This may be due to the fact that there is almost no transfer of heat between the phases and therefore the values of R_{Dc} remain unaltered by the properties of the solid phase. For larger values of H_t, the condition for the occurrence of instability is based on the mean properties of the medium and therefore R_{Dc} turns out to be dependent on γ. From Fig. 5(*a*), it is also noted that the effect of increasing γ has a destabilizing effect on the system. This is because an increase in the value of γ leads to significant transfer of heat through both solid and fluid phases which in turn reduces the stabilizing effect of the interphase heat-transfer coefficient. The critical wave number (Fig. 5(*b*)) attains the same value as $H_t \to 0$ and $H_t \to \infty$ for all values of γ considered and a

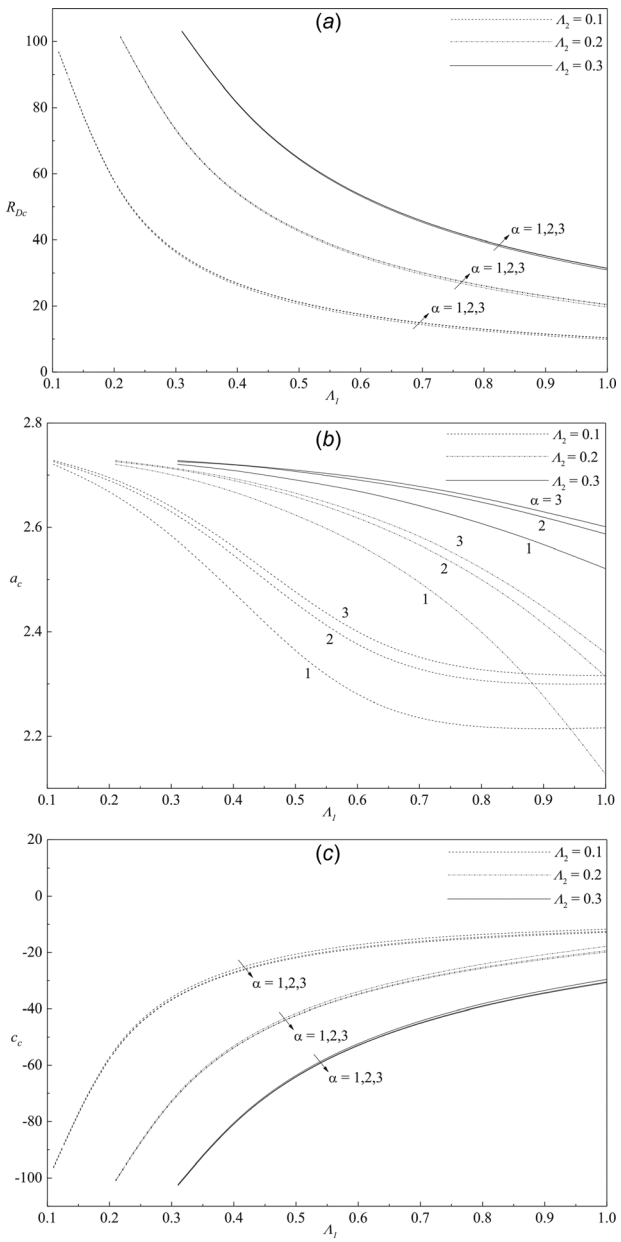

Fig. 7 Variation of (*a*) R_{Dc}, (*b*) a_c, and (*c*) c_c with Λ_1 for various values of α and Λ_2 when $H_t = 20$, $\gamma = 0.5$

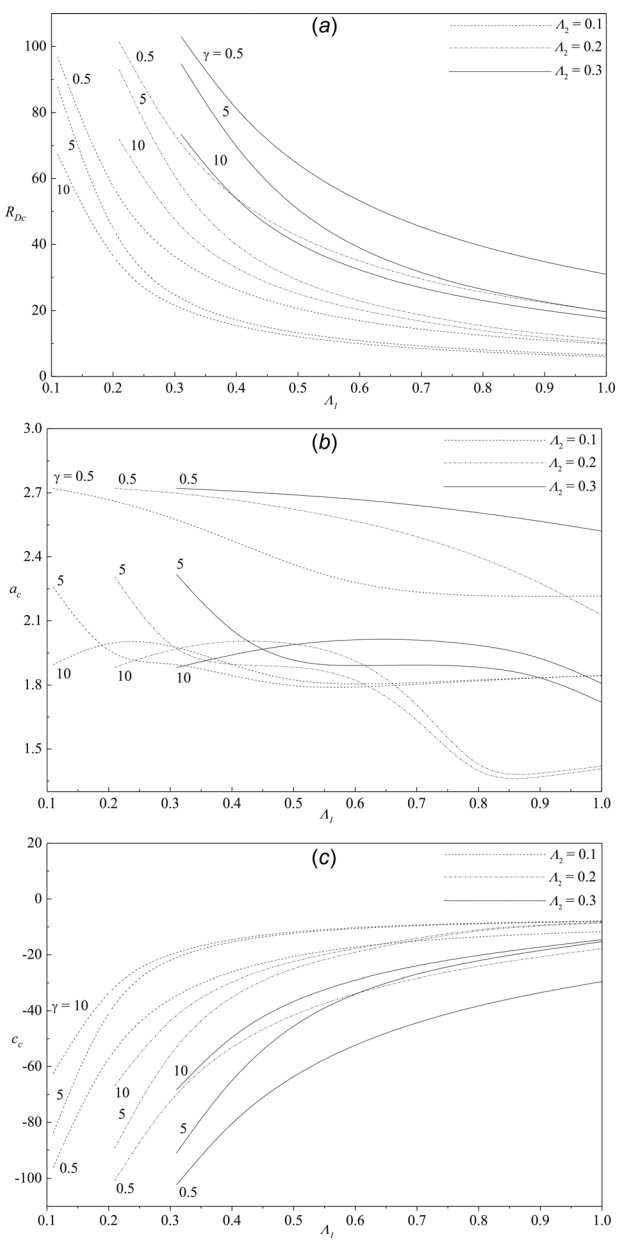

Fig. 8 Variation of (*a*) R_{Dc}, (*b*) a_c, and (*c*) c_c with Λ_1 for various values of γ and Λ_2 when $H_t = 20$, $\alpha = 1$

similar behavior could be seen in the case of critical wave speed (Fig. 5(*c*)). Furthermore, a_c attains both maximum as well as minimum value and c_c passes through a minimum value at intermediate values of H_t.

Figures 6(*a*)–6(*c*), 7(*a*)–7(*c*), and 8(*a*)–8(*c*) show the variation of triplets (R_{Dc}, a_c, c_c) as a function of Λ_1 for different values of Λ_2, H_t, α, and γ. These figures indicate that Λ_1 and Λ_2 have destabilizing and stabilizing influence on the system, respectively, while increasing H_t (Fig. 6(*a*)), α (Fig. 7(*a*)) and decreasing γ (Fig. 8(*a*)) exhibit stabilizing effect on the flow for a fixed value of Λ_2. Although the effect of α is to reinforce stability on the system due to decrease in the value of heat capacity of the fluid, its influence on the stability characteristics is found to be marginal. The effect of increasing H_t (Fig. 6(*b*)) and α (Fig. 7(*b*)) increases the critical wave number but shows a mixed behavior with the increase in γ (Fig. 8(*b*)). Moreover, increasing Λ_1 is to increase the size of convection cells while an opposite trend is observed with increasing Λ_2. The critical wave speed shown in Figs. 6(*c*), 7(*c*) and 8(*c*) reveals that c_c increases as Λ_1 increases but a reverse inclination is observed with the increase in Λ_2. Also, increasing H_t (Fig. 6(*c*)), α (Fig. 7(*c*)) and decreasing γ (Fig. 8(*c*)) is to decrease the critical wave speed.

6 Conclusions

The effect of local thermal nonequilibrium (LTNE) on the linear stability of natural convection in a vertical porous layer has been investigated with impermeable and isothermal boundaries. The saturating fluid is assumed to be viscoelastic of an Oldroyd-B type. A modified Darcy's law is utilized to describe the flow in a porous medium and a two field temperature model representing fluid and solid phases separately is used. The governing dimensionless parameters influencing the stability of the system are the Darcy–Rayleigh number, R_D, scaled interphase heat transfer coefficient, H_t, relaxation parameter, Λ_1, retardation parameter, Λ_2, porosity-modified conductivity ratio, γ, and the diffusivity ratio α. It has been shown, using the method of Gill [1], that stability is not guaranteed when viscoelastic effects are present. Hence, the eigenvalue stability problem has been solved numerically for a wide range of parametric values. Despite the basic state remains the same for viscoelastic and Newtonian fluids, the system becomes unstable via oscillatory mode in the case of viscoelastic fluids; a result which is qualitatively different from Newtonian fluids. It is also observed that the system is always stable only when $\Lambda_1 = \Lambda_2$ (Newtonian fluid) but not as $\Lambda_1 \to 0$ (with $\Lambda_2 = 0$). The influence of viscoelastic parameters Λ_1 and Λ_2 on the stability of the system is found to be opposite in nature and they display destabilizing and stabilizing effects, respectively. Intriguingly, the effect of increasing H_t and α is found to be stabilizing while increasing γ displays a destabilizing effect on the base flow. The critical wave number assumes the same value at lower and higher values of H_t irrespective of the values of physical parameters involved therein. The results for the Maxwellian fluid are obtained as a particular case from the present study and observed that the system is more unstable for such type of viscoelastic fluids.

Acknowledgment

The authors acknowledge with thanks Professor D.A.S. Rees for providing the translated (Russian to English) version of the paper of Alishaev and Mirzadjanzade [29]. We thank the anonymous referees for their constructive comments, which helped us to improve the quality of manuscript considerably. One of the authors B.M.S wishes to thank the authorities of his University for the encouragement and support.

Nomenclature

a = vertical wave number
c = wave speed
c_i = growth rate
c_r = phase velocity
d = thickness of the fluid layer
$\mathbf{g}$ = acceleration due to gravity
h = interphase heat transfer coefficient
H_t = scaled interphase heat transfer coefficient
k = unit vector in z-direction
K = permeability
p = pressure
P = modified pressure
$\mathbf{q} = (u, v, w)$ = velocity vector
R_D = Darcy–Rayleigh number
t = time
T_f = temperature of the fluid
T_s = temperature of the solid
T_1 = temperature of the left boundary
T_2 = temperature of the right boundary
(x, y, z) = Cartesian co-ordinates

Greek Symbols

α = diffusivity ratio
β = thermal expansion coefficient
γ = porosity-modified conductivity ratio
ε = porosity of the medium
θ = fluid temperature
Θ = disturbance fluid temperature
κ = thermal diffusivity
λ_1 = stress relaxation
λ_2 = strain relaxation
Λ_1 = relaxation parameter
Λ_2 = retardation parameter
μ = fluid viscosity
ρ_f = fluid density
ρ_0 = reference density at T_0
ϕ = solid temperature
Φ = disturbance solid temperature
ψ = stream function
Ψ = disturbance stream function

Subscripts

b = basic state
f = fluid phase
s = solid phase

Appendix A

The resulting eigenvalue problem has also been solved using the Galerkin method. Accordingly, $\Psi(x), \Theta(x)$, and $\Phi(x)$ are expanded in terms of Legendre polynomials in the form

$$\Psi(x) = \sum_{n=0}^{N} a_n \xi_n(x), \quad \Theta(x) = \sum_{n=0}^{N} b_n \xi_n(x), \quad \Phi(x) = \sum_{n=0}^{N} c_n \xi_n(x) \tag{A1}$$

with the corresponding base functions

$$\xi_n(x) = (1 - x^2) P_n(x) \tag{A2}$$

where $P_n(x)$ is the Legendre polynomial of degree n and a_n, b_n, and c_n are constants. It may be noted that $\Psi(x), \Theta(x)$, and $\Phi(x)$ satisfy the boundary conditions. Equation (A1) is substituted into Eqs. (21)–(23) and the resulting error is required to be orthogonal to $\xi_m(x)$ for $m = 0, 1, 2, \ldots N$. This gives

$$\sum_{n=0}^{N} a_n \int_{-1}^{1} (\xi_n' \xi_m' + a^2 \xi_n \xi_m)\, dx + R_D \sum_{n=0}^{N} b_n \int_{-1}^{1} \xi_n' \xi_m dx = iac\Lambda_2 \sum_{n=0}^{N} a_n \int_{-1}^{1} (\xi_n' \xi_m' + a^2 \xi_n \xi_m) dx + iac\Lambda_1 R_D \sum_{n=0}^{N} b_n \int_{-1}^{1} \xi_n' \xi_m dx \tag{A3}$$

$$ia\sum_{n=0}^{N} a_n \int_{-1}^{1} \xi_n \xi_m\, dx - \sum_{n=0}^{N} b_n \int_{-1}^{1} (\xi_n' \xi_m' + a^2 \xi_n \xi_m) dx - H_t \sum_{n=0}^{N} b_n \int_{-1}^{1} \xi_n \xi_m dx - iaR_D \sum_{n=0}^{N} b_n \int_{-1}^{1} x \xi_n \xi_m dx + H_t \sum_{n=0}^{N} c_n \int_{-1}^{1} \xi_n \xi_m dx = -iac \sum_{n=0}^{N} b_n \int_{-1}^{1} \xi_n \xi_m dx \tag{A4}$$

$$H_t\gamma \sum_{n=0}^{N} b_n \int_{-1}^{1} \xi_n \xi_m\, dx - \sum_{n=0}^{N} c_n \int_{-1}^{1} (\xi_n' \xi_m' + a^2 \xi_n \xi_m) dx - H_t\gamma \sum_{n=0}^{N} c_n \int_{-1}^{1} \xi_n \xi_m dx = -iac\alpha \sum_{n=0}^{N} c_n \int_{-1}^{1} \xi_n \xi_m dx \tag{A5}$$

in which the primed quantities denote differentiation with respect to x. The above equations form the following system of linear algebraic equations:

$$AX = cBX \tag{A6}$$

Appendix B

Following the energy stability analysis adopted by Rees [20], Eqs. (22) and (23) are used to determine Ψ in terms of Θ and Φ, and substitute it into Eq. (21). This gives the following two equations:

$$\Theta'''' - 2a^2\Theta'' + a^4\Theta + H_t(\Phi'' - a^2\Phi) - H_t(\Theta'' - a^2\Theta) + iaR_D\left[\left(\frac{1 - ia\Lambda_1 c}{1 - ia\Lambda_2 c}\right)\Theta' - (x\Theta)'' + a^2 x\Theta\right] = -iac(\Theta'' - a^2\Theta) \tag{B1}$$

$$\Phi'''' - 2a^2\Phi'' + a^4\Phi - H_t\gamma(\Phi'' - a^2\Phi) + H_t\gamma(\Theta'' - a^2\Theta) = -ia\alpha c(\Phi'' - a^2\Phi) \tag{B2}$$

We now multiply Eqs. (B1) and (B2) by $\gamma\,\bar{\Theta}$ and $\bar{\Phi}$, respectively, and integrate the resulting equations over the channel width and sum the ensuing integrals. This procedure gives the following:

$$\int_{-1}^{1} \left[\gamma\left(|\Theta''|^2 + 2a^2|\Theta'|^2 + a^4|\Theta|^2\right) + \left(|\Phi''|^2 + 2a^2|\Phi'|^2 + a^4|\Phi|^2\right)\right] dx + H_t\gamma \int_{-1}^{1} \left(|\Theta' - \Phi'|^2 + a^2|\Theta - \Phi|^2\right) dx + ia\gamma R_D \times \left[\left(\frac{1 - iac\Lambda_1}{1 - iac\Lambda_2}\right) \int_{-1}^{1} \Theta'\bar{\Theta} dx - \int_{-1}^{1} (x\Theta)''\bar{\Theta}\, dx + a^2 \int_{-1}^{1} x|\Theta|^2 dx\right] = iac \int_{-1}^{1} \left[\gamma\left(|\Theta'|^2 + a^2|\Theta|^2\right) + \alpha\left(|\Phi'|^2 + a^2|\Phi|^2\right)\right] dx \tag{B3}$$

Equating the real part on both sides of Eq. (B3), we get

$$a^2\gamma c_r R_D \left[\frac{\Lambda_1 - \Lambda_2}{a^2 c_r^2 \Lambda_2^2 + (1 + ac_i\Lambda_2)^2}\right] \int_{-1}^{1} \Theta'\bar{\Theta} dx + H_t\gamma \int_{-1}^{1} \left[|\Theta' - \Phi'|^2 + a^2|\Theta - \Phi|^2\right] dx + \int_{-1}^{1} \left[\gamma\left(|\Theta''|^2 + 2a^2|\Theta'|^2 + a^4|\Theta|^2\right) + \left(|\Phi''|^2 + 2a^2|\Phi'|^2 + a^4|\Phi|^2\right)\right] dx = -ac_i \int_{-1}^{1} \left[\gamma\left(|\Theta'|^2 + a^2|\Theta|^2\right) + \alpha\left(|\Phi'|^2 + a^2|\Phi|^2\right)\right] dx \tag{B4}$$

From Eq. (B4), it is evident that the stability of the system cannot be ascertained, in general, for viscoelastic fluids as the value of c_i cannot be fixed and hence Rees's proof of stability becomes ineffective in the present case. Nonetheless, for the case of Newtonian fluid ($\Lambda_1 = \Lambda_2$), it is noted that c_i is negative always and hence the system is stable; a result established by Rees [20].

References

[1] Gill, A. E., 1969, "A Proof That Convection in a Porous Vertical Slab is Stable," J. Fluid Mech., **35**(03), pp. 545–547.
[2] Rees, D. A. S., 1988, "The Stability of Prandtl–Darcy Convection in a Vertical Porous Slot," Int. J. Heat Mass Transfer, **31**(7), pp. 1529–1534.
[3] Lewis, S., Bassom, A. P., and Rees, D. A. S., 1995, "The Stability of Vertical Thermal Boundary Layer Flow in a Porous Medium," Eur. J. Mech. B, **14**(4), pp. 395–408.
[4] Straughan, B., 1988, "A Nonlinear Analysis of Convection in a Porous Vertical Slab," Geophys. Astrophys. Fluid Dyn., **42**(3–4), pp. 269–275.
[5] Qin, Y., and Kaloni, P. N., 1993, "A Nonlinear Stability Problem of Convection in a Porous Vertical Slab," Phys. Fluids A, **5**(8), pp. 2067–2069.
[6] Barletta, A., and de B. Alves, L. S., 2014, "On Gill's Stability Problem for Non-Newtonian Darcy's Flow," Int. J. Heat Mass Transfer, **79**, pp. 759–768.
[7] Vafai, K., and Sozen, M., 1990, "Analysis of Energy and Momentum Transport for Fluid Flow Through a Porous Bed," ASME J. Heat Transfer, **112**(3), pp. 690–699.
[8] Minkowycz, W. J., Haji-Sheikh, A., and Vafai, K., 1999, "On Departure From Local Thermal Equilibrium in Porous Media Due to a Rapidly Changing Heat Source: the Sparrow Number," Int. J. Heat Mass Transfer, **42**(18), pp. 3373–3385.
[9] Duval, F., Fichot, F., and Quintard, M., 2004, "A Local Thermal Non-Equilibrium Model for Two-Phase Flows With Phase-Change in Porous Media," Int. J. Heat Mass Transfer, **47**(3), pp. 613–639.
[10] Rees, D. A. S., and Pop, I., "Local Thermal Non-Equilibrium in Porous Medium Convection," *Transport Phenomena in Porous Media III*, D. B. Ingham and I. Pop, eds., Elsevier, Oxford, UK, pp. 147–173.
[11] Rees, D. A. S., 2010, "Microscopic Modelling of the Two-Temperature Model for Conduction in Heterogeneous Media," J. Porous Media, **13**(2), pp. 125–143.
[12] Nield, D. A., and Bejan, A., 2013, *Convection in Porous Media*, 4th ed., Springer, New York.
[13] Banu, N., and Rees, D. A. S., 2002, "Onset of Darcy–Benard Convection Using a Thermal Non-Equilibrium Model," Int. J. Heat Mass Transfer, **45**(11), pp. 2221–2228.
[14] Malashetty, M. S., Shivakumara, I. S., and Kulkarni, S., 2005, "The Onset of Lapwood–Brinkman Convection Using a Non-Equilibrium Model," Int. J. Heat Mass Transfer, **48**(6), pp. 1155–1163.
[15] Shivakumara, I. S., Malashetty, M. S., and Chavaraddi, K. B., 2006, "Onset of Convection in a Viscoelastic Fluid Saturated Sparsely Packed Porous Layer Using a Thermal Non-Equilibrium Model," Can. J. Phys., **84**(11), pp. 973–990.
[16] Straughan, B., 2010, "Green-Naghdi Fluid With Non-Thermal Equilibrium Effects," Proc. R. Soc. A, **466**(2119), pp. 2021–2032.
[17] Celli, M., Barletta, A., and Storesletten, L., 2013, "Thermoconvective Instability and Local Thermal Non-Equilibrium in a Porous Layer With Isoflux-Isothermal Boundary Conditions," 31st UIT Heat Transfer Conference, Como, Italy, June 25–27, pp. 45–53.
[18] Barletta, A., and Rees, D. A. S., 2015, "Local Thermal Non-Equilibrium Analysis of the Thermoconvective Instability in an Inclined Porous Layer," Int. J. Heat Mass Transfer, **83**, pp. 327–336.
[19] Barletta, A., Celli, M., and Lagziri, H., 2015, "Instability of a Horizontal Porous Layer With Local Thermal Non-Equilibrium: Effects of Free Surface and Convective Boundary Conditions," Int. J. Heat Mass Transfer, **89**, pp. 75–89.
[20] Rees, D. A. S., 2011, "The Effect of Local Thermal Nonequilibrium on the Stability of Convection in a Vertical Porous Channel," Transp. Porous Media, **87**(2), pp. 459–464.

[21] Scott, N. L., and Straughan, B., 2013, "A Nonlinear Stability Analysis of Convection in a Porous Vertical Channel Including Local Thermal Non-equilibrium," J. Math. Fluid Mech., **15**(1), pp. 171–178.
[22] Straughan, B., 2015, *Convection With Local Thermal Nonequilibrium and Microfluidic Effects*, Springer, Heidelberg.
[23] Malashetty, M. S., Tan, W., and Swamy, M., 2009, "The Onset of Double Diffusive Convection in a Binary Viscoelastic Fluid Saturated Anisotropic Porous Layer," Phys. Fluids, **21**(8), p. 084101.
[24] Li, Z., and Khayat, R. E., 2005, "Finite-Amplitude Rayleigh–Benard Convection and Pattern Selection for Viscoelastic Fluids," J. Fluid Mech., **529**, pp. 221–251.
[25] Sheu, L. J., Tam, L. M., Chen, J. H., Chen, H. K., Lin, K. T., and Kang, Y., 2008, "Chaotic Convection of Viscoelastic Fluids in Porous Media," Choas Solitons Fractals, **37**(1), pp. 113–124.
[26] Malashetty, M. S., and Kulkarni, S., 2009, "The Convective Instability of Maxwell Fluid-Saturated Porous Layer Using a Thermal Non-Equilibrium Model," J. Non-Newtonian Fluid Mech., **162**(1–3), pp. 29–37.
[27] Gozum, D., and Arpaci, V. S., 1974, "Natural Convection of Viscoelastic Fluids in a Vertical Slot," J. Fluid Mech., **64**(03), pp. 439–448.
[28] Takashima, M., 1993, "The Stability of Natural Convection in a Vertical Layer of Viscoelastic Liquid," Fluid Dyn. Res., **11**(4), pp. 139–152.
[29] Alishaev, M. G., and Mirzadjanzade, A. Kh., 1975, "For the Calculation of Delay Phenomenon in Filtration Theory," Izvestya Vuzov Nefti Gaz. **6**, pp. 71–78.
[30] Khuzhayorov, B., Auriault, J. L., and Royer, P., 2000, "Derivation of Macroscopic Filtration Law for Transient Linear Viscoelastic Fluid Flow in Porous Media," Int. J. Eng. Sci., **38**(5), pp. 487–504.
[31] Akhatov, I. Sh., and Chembarisova, R. G., 1993, "The Thermoconvective Instability in Hydrodynamics of Relaxational Liquids," *Instabilities in Multiphase Flows*, G. Gouesbet and A. Berlemont, eds., Plenum Press, New York.
[32] Bird, R. B., Stewart, W. E., and Lightfoot, E. N., 2007, *Transport Phenomena*, Wiley, New York.
[33] Hirata, S. C., de B. Alves, L. S., Delenda, N., and Ouarzazi, M. N., 2015, "Convective and Absolute Instabilities in Rayleigh–Bénard–Poiseuille Mixed Convection for Viscoelastic Fluids," J. Fluid Mech., **765**, pp. 167–210.